Study of Properties of AlN Thin Films Deposited by Reactive Magnetron Sputtering

Neelam Kumari
Department of Applied Physics, BIT, Mesra, Ranchi-835215, India, neelamjha_nj@yahoo.co.in

Ashwini K. Singh
Department of Applied Physics, BIT, Mesra, Ranchi-835215, India, neelamjha_nj@yahoo.co.in

P.K. Barhai
Department of Applied Physics, BIT, Mesra, Ranchi-835215, India, neelamjha_nj@yahoo.co.in

Follow this and additional works at: https://digitalcommons.aaru.edu.jo/ijtfst

Study of Properties of AlN Thin Films Deposited by Reactive Magnetron Sputtering

Neelam Kumari[*], Ashwini K. Singh and P.K. Barhai

Department of Applied Physics, BIT, Mesra, Ranchi-835215, India
[*] *E-mail: neelamjha_nj@yahoo.co.in*

Abstract: Study of Aluminum nitride (AlN) thin film deposited on silicon wafer and glass substrates by DC magnetron sputtering technique at different power variation. The X-ray diffraction and Fourier transform infrared spectroscopy (FTIR) study revealed the formation of the AlN phase. The optical characteristics of films, such as refractiveindex, extinction coefficient, and average thickness, were calculated by Swanepoel's method using transmittance measurements. The refractiveindex and average roughness values of the films increased with film thickness. At lower power (100W) and constant gas ratio the film surface roughness was 1.7 nm. It was observed that films coated at lower power were 75% transparent in the visible spectral region.

Keywords: Magnetron sputtering, Thin film, Deposition rate, Transmittance

1. INTRODUCTION

Aluminium nitride (AlN) is a wide band-gap (6.2 eV) [1-3] III–V compound, which has attracted attention of the scientific community due to its exotic properties. Thin film of AlN with a hexagonal wurtzite crystalline structure is used in various applications like optical hard coatings, wear resistant, high temperature microelectronics, chemical and thermal stability [4-7]. Its high thermal conductivity ($180 Wm^{-1}K^{-1}$) [8, 9], excellent piezoelectricity [10], high electrical resistivity ($\rho = 10^9 – 10^{11}\Omega m$) [11], and fast acoustic velocity [12] make AlN promising material for use in optoelectronic, surface acoustic wave devices, sensor and thin film resonators [13, 14]. Thermal conductive AlN films with moderate dielectric constant are considered for metal-oxide-semiconductor (MOS) applications [15]. AlN films are used for optical applications in corrosive and high temperature environments [16, 17].

Quality AlN thin film requires high purity source and oxygen free environment for deposition because of the aluminium reactivity. Traditionally, AlN films are deposited by various techniques, preferably chemical vapour deposition (CVD) or molecular beam epitaxy (MBE) [18-21], pulsed laser deposition (PLD) [22-24] and electron shower method [25]. Recently, many reports on low temperature deposition of good quality AlN films by physical vapour deposition (PVD) techniques are available. In the PVD process DC reactive magnetron sputtering is the most common deposition process. Among these, sputtering has advantages over other conventionally used high temperature techniques because of its simplicity, low thermal temperature, low cost and its ability to produce good quality films with desired properties [26-27]. Characteristic features of the prepared films depend on the processing parameters and method and are easier to control in PVD process.

In this work the AlN- films are deposited on Si and glass substrates by the DC reactive magnetron sputtering. To achieve the desired property we observed the effects of power on the phase, structure, and film formation on Si and glass substrates. All the deposition is carried out keeping constant gas ratio, deposition temperature and the base pressure. The thin films are characterized using X-ray diffraction (XRD), Atomic Force Microscopy (AFM), spectroscopic Ellipsometer. Optical properties of the films are analysed using UV-Visible spectrometer and Fourier Transform Infrared (FTIR) Spectroscopy. The optical properties of thin films have been investigated by various analytical and numerical methods [28-31]. In these methods, transmittance and reflectance data have been used to calculate thin film optical constants, such as refractive index $n(\lambda)$, extinction coefficient $k(\lambda)$, and film thickness d.

2. EXPERIMENTAL DETAILS

2.1 Deposition

A schematic diagram of the DC magnetron Sputtering deposition system is shown in Fig 1. The DC magnetron sputtering system consists of a vacuum chamber, cathode (connected to 1kV DC power supply), mass flow controller, sample holder and view port. Pure Al target

(50 mm diameter, 5 mm thick, 99.99% pure) was mechanically clamped to the magnetron cathode of the sputtering system.
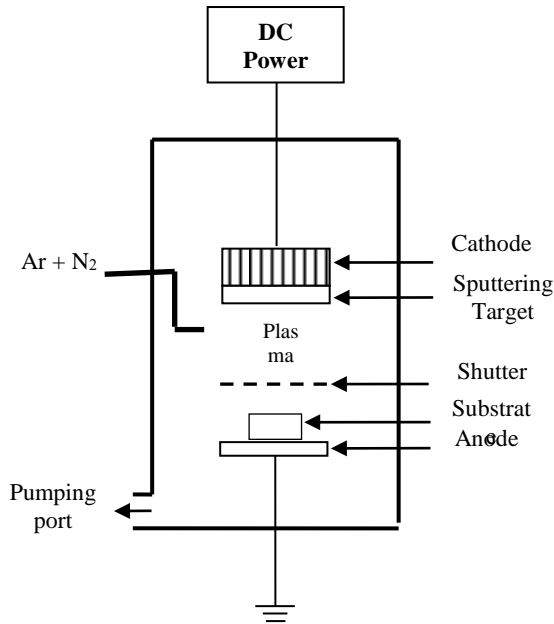

Figure 1. Schematic Diagram of DC Magnetron Sputtering System

Silicon substrates of size 10 X 10 mm² were obtained by cutting silicon wafers of thickness ~ 0.5 mm and glass of thickness ~ 3mm. The substrates were ultrasonically cleaned and dried at room temperature prior to deposition. Substrates were mounted on the sample holder and a base pressure of ~10^{-6} mbar was obtained. The target surface was sputter etched by Ar at 100 W for 20 min to avoid contamination before deposition. After sputter cleaning, Ar: N_2 gas flow rate was adjusted to 4: 6 ratios and working pressure of ~ 2 x 10^{-2} mbar was maintained during deposition. In this way, films were obtained at four different DC power (100, 200, 300 and 400 W). The substrate temperature was monitored using a thermocouple. Film growth conditions are summarized in Table 1.

Table 1: Deposition Parameters for AlN (D.C. reactive Sputtering)

Objects	Specification
Target	Al pure (99.99%)
Substrate	Si wafer and glass
Target to substrate distance	6.5cm
DC power	100, 200, 300 and 400 W
Substrate temperature	Room- Temperature
Sputtering time	60 minute

Thickness of the films was measured using ellipsometer (Nano- View Inc., Korea; SEMG1000-VIS) with instrumental error of ± 6 nm error bar. The thickness of each sample is represented by ± 6 nm error bar. Crystallographic analysis of the deposited films was done by GIXRD(Model: Bruker D8 Advance X-ray diffractometer). The x- rays were produced using a sealed tube and the wavelength of x-ray was 0.154 nm (Cu K-alpha). The x-rays were detected using a fast counting detector based on Silicon strip technology (Bruker Lynx Eye detector). Surface morphology of the films was investigated by an AFM. Al-N bond formation was characterized by FTIR spectroscopy (Shimadzu Corpn., IR-Prestige). Optical transmission spectra (Perkin Elmer, Lambda-25) of these AlN films were measured at room temperature from 190 to 800 nm in wavelength region using a dual-beam spectrophotometer. The film surface resistivity was measured using standard four-point probe method. The resistivity was calculated using Van der Pauw method. According to which the resistivity is given by, ρ = (k x V x t) / I, where k = CF1 x CF2; CF1 and CF2 are the two geometric correction factors, V/I is the slope of plot obtained by four point probe measurements and t is the film thickness. In our study, the applied correction factor (k) is taken as 0.95 [32]. To minimize the experimental error resistivity measurement was taken at different places on film surface.

2.2 Optical Properties measurement

A homogeneous thin film deposited on a transparent substrate with a thickness of several orders of magnitude greater than that of the film. The film and the substrate are surrounded by air with a refractive index $n_0 \approx 1$ and the incident light from the spectrophotometer is normal to the substrate. The film has a complex refractive index given by:

N = n – ik,

Where, n = refractive index, k = extinction coefficient
Extinction coefficient is expressed in terms of the absorption coefficient 'α' by:

$$k = \frac{\alpha \lambda}{4\pi}, \qquad (1)$$

Where, λ = wavelength
The transmission spectrum contains interference fringes that obey the basic formula

$$2nd = m\lambda, \qquad (2)$$

Where
m = interference order is an integer for maxima and a half- integer for minima in the transmission spectrum
d = film thickness.
The transmission spectrum roughly divided into three regions:
the transparent region: (α = 0),
the weak and medium absorption region where α is small, and
the strong absorption region where the transmission decreases markedly owing to the effect of α.
For the case of $k^2 \ll n^2$, the transmittance T for normal incidence is given by [29]

$$T = \frac{Ax}{B - Cx \cos\varphi + Dx^2} \qquad (3)$$

With
A = 16 n^2 s,
B = $(n+1)^3 (n+ s^2)$,
C = $2(n^2-1)(n^2- s^2)$

$\Phi = 4\pi \frac{nd}{\lambda}$,
D = $(n-1)^3 (n-s^2)$,
x = exp $(-\alpha d)$.

The transmission values at the extremes of the interference fringes can be obtained using eq. (2) by substituting cos φ = +1 and -1 for maxima and minima respectively. Thus, eq. (2) can be written as

$$T_M = \frac{Ax}{B-Cx+Dx^2} ,$$ (3a)

$$T_m = \frac{Ax}{B+Cx+Dx^2} .$$ (3b)

In the medium and weak absorption region, the refractive index of the film can be calculated as [29]

$$n_i = [N + (N^2 - s^2)^{1/2}]^{1/2,}$$ (4a)

For which

$$N = 2s \frac{T_M - T_m}{T_M T_m} + \frac{s^2 + 1}{2}$$ (4b)

Here, T_M and T_m are the transmission maximum and the corresponding minimum at a certain wavelength λ_i, respectively. Alternatively, one of these values is an experimental interference extreme and the other one is derived from the corresponding envelope. The substrate refractive index and the film thickness are s and d, respectively. The first approximate value of the film thickness is given by

$$d_i = \frac{\lambda_i \lambda_{i+1}}{2(\lambda_i n_{i+1} - \lambda_{i+1} n_i)},$$ (5)

Where n_i and n_{i+1} are the refractive indices at two adjacent maxima at λ_i and λ_{i+1}, respectively. The substrate refractive index s is evaluated as

$$S = \frac{1}{T_s} + \left(\frac{1}{T_s^2} - 1\right)^{\frac{1}{2}}$$ (6)

Where Ts is the substrate transmittance, which is almost a constant in the transparent region. The first approximate value of the film thickness $\bar{d}_1$ is the average value of d_i. This value is used, together with n_i, to calculate the ''order number'' m_0 for the different extremes using eq. (1). The accuracy of the film thickness is increased by taking the corresponding exact integer values of m associated with each extreme point, resulting in a new thickness, d_2, from eq. (1). The new thickness values should have a much smaller dispersion and their average is taken as the film final thickness $\bar{d}_2$. The root mean-squared deviation of different d_2 values is

considered in our case to determine the accuracies of the final thickness, which are approximately 3 and 2% for samples 100 and 200W, respectively. By using the average value of film thickness $\bar{d}_2$ and the exact value of m, the final values of the refractive index n are obtained. Moreover, the values of n can be fitted to a reasonable function, such as the two-term Cauchy dispersion relation, which can be used for extrapolation at all wavelengths and is well suited to the transparent materials through the following relationship [33].

$$n(\lambda) = a + \frac{b}{\lambda^2} ,$$ (7)

Where a and b are the fitting parameters and λ is give in nm.

The accuracy of the optical constant determination is strongly affected by the amplitude of transmission oscillation [34]. There are two necessary conditions required for good fringe patterns: 1) the difference between n and s should be as large as possible and 2) the thickness of the glass substrate should be several orders of magnitude higher than the film thickness. The relative error in the refractive index is given by [34]

$$\frac{\Delta n}{n} = \frac{\Delta T}{T}\left(\frac{T_M + T_m}{T_M - T_m}\right)\frac{1}{f(n,s)},$$ (8)

Where

$$f(n,s) = -2\frac{(n^2-s)(n^2+s)}{(n^2-1)(n^2-s^2)},$$ (9)

And ΔT/T is the relative precision measurement.

The accuracy is strongly affected by the presence of the ratio $(T_M + T_m)/ (T_M - T_m)$, especially in the case of a low amplitude of transmission oscillation [34].

3. RESULTS & DISCUSSIONS

Thin film depends on the kinetics of the arrival species at the substrate and is directly dependent on the deposition parameters. The deposition parameters are summarized in Table I. On increasing the DC power cathode current increases and thicker films are obtained. It is due to the reason that at higher DC values number of electrons supplied into the plasma is increased and coating parameter supported the better film formation with minimum re-sputtering [35]. Graph of film thickness and supplied voltage confirms the expected increase in thickness (Fig. 2). The XRD pattern of AlN thin films deposited at various DC powers from 100 to 400 W is shown in Fig. 3.
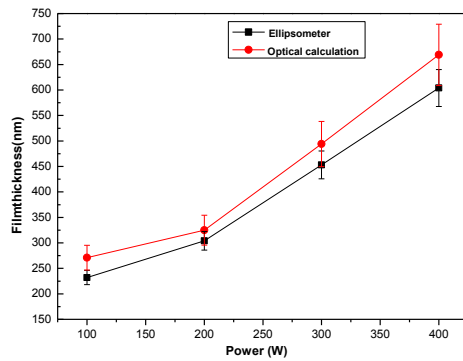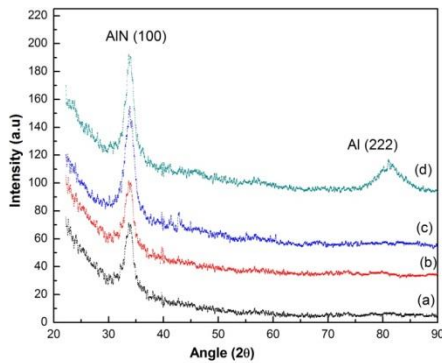
Figure 2. Film thickness of AlN films on DC power

Figure 3. GIXRD diffractograms of deposited filmsprepared at different DC power; (a) 100W, (b) 200W,(c) 300W, and (d) 400W.

2d image

3d image

Fig. 4. (a) 2-D and (b) 3-D AFM image of topography of AlN thin films deposited at 100 W.

The XRD spectra of the deposited films were confirmed using the JCPDS data tables. It shows that diffraction peaks observed at $2\theta = 33.310$ correspond to (100) AlN (JCPDS card No. 79-2497) is prominent and stronger with increasing power from 100 to 400 W. When the power was increased to 400 W (Fig. 3(d)), extra peak observed at $2\theta = 82.320$ that corresponds to Al (222) phase (JCPDS card No. 85-1327). This extra phase of Al in the XRD spectra isdue to the excess Al atoms ejected from the target at higher DC power, which were not reacted and deposited in pure form on the substrate.

The surface topography of AlN thin films is characterized by AFM. Fig. 4 is two and three dimensional AFM image of 150 nm×150 nm deposited at 100W. Overall smooth and uniform AlN film surface is found at these growth conditions. Fig. 5 shows the root mean square (RMS) surface roughness derived from the corresponding AFM images. The surface roughness of the AlN films increases with the increase of the DC power. Kajikawa et al. studied the correlation between process conditions and film structure, and suggested that the morphology of reactive-sputtered nitride films can be affected at both initial and growth stages. In the initial stage, four processes occur, which include (I) nucleation due to epitaxial relationship or due to
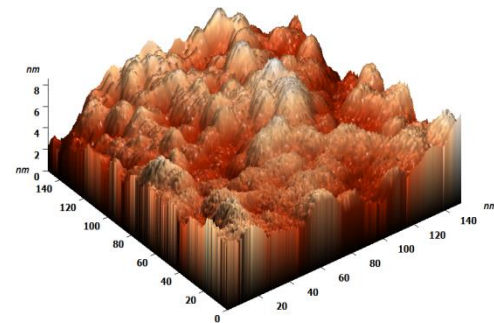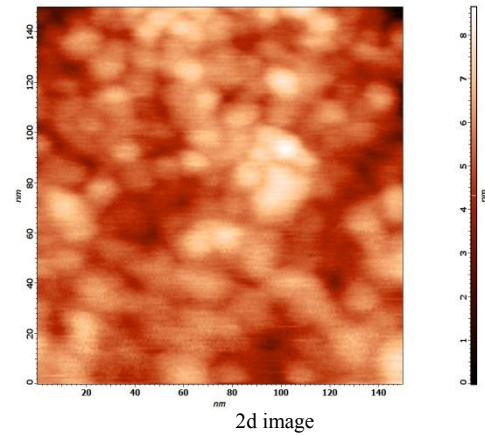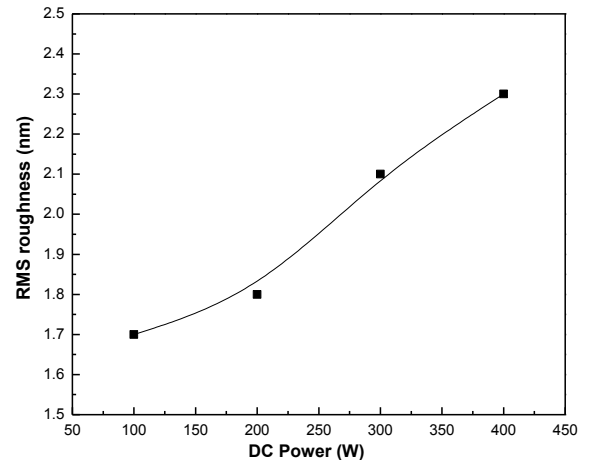

Fig. 5. Variation of the AlN surface roughness as a function of the DC power.

surface and interfacial energy anisotropy, (II) coarsening due to surface and interfacial energy anisotropy, (III) grain growth, and (IV) resputtering due to ion bombardment. In the growth stage, three processes occur

at the surface, including (I) precursor sticking, (II) surface diffusion of adatoms, and (III) resputtering due to ion bombardment [36]. Since nitride film formation during reactive sputtering occur at the substrate and deposited surface, Increase in the plasma power may have resulted in increasing the number of ejected Al species from the target, which results in the increase of film thickness with the increasing DC power as shown in Fig. 2. On the other hand, the incident energy of the high energetic ions will contribute to the surface migration and surface reaction to form a flat surface, which leads to the increase of the RMS surface roughness with increasing the DC power as observed in Fig. 5.

Fig. 6 shows the wavelength dependence of optical transmittance of the AlN films grown at different DC

Figure 7. Variation of refractive index (n) versus wavelength (λ) for AlN films at 100 and 200 W.

In Fig. 7 the variation in refractive index as a function of wavelength for samples 100 W and 200W. We observed that the refractive index initially decreases with increase in wavelength and finally becomes constant at a higher wavelength. We found that the refractive index of 100 W samples in the range of 1.67 to 1.74 and for 200 W the range is 1.79 to 2.12. It had been observed that with increase in thickness refractive index increases at the cost of film transparency and surface roughness. Film roughness results in scattering, as roughness increases scattering increases and hence films become less transparent. Refractive index of 100W sample calculated at 550nm is 1.64 and extinction coefficient in the visible range is $k = 5 \times 10^{-3}$. Film thickness at same power using Swanepoel's method is 271 ± 9 nm.

FTIR spectroscopy was used for the investigation of Al-N bond (Fig. 8). FTIR in ATR (Attenuated Total Reflectance) mode was used in which spectra is swept in between 650 to 4000 cm^{-1}. Two prominent peaks 754 and 883 cm^{-1} observed in the spectra which correspond to Al-N bond that is absorption band of AlN nanoparticles [37, 38].
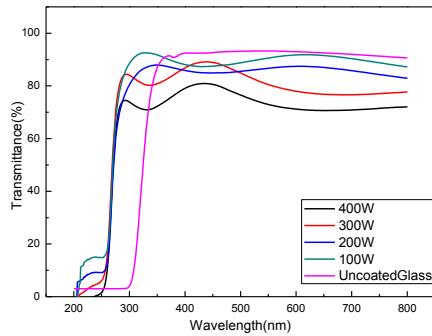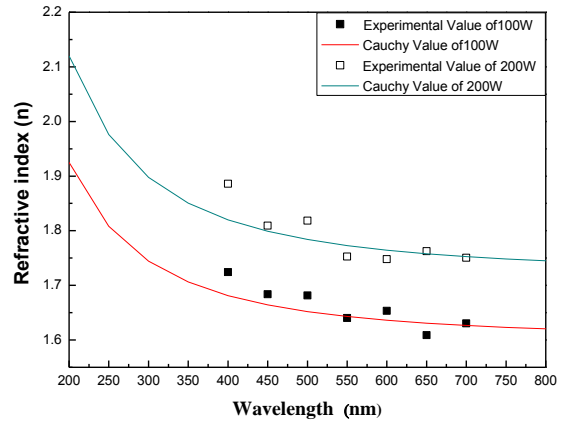

Fig. 6: Optical transmittance spectra of AlN grown under various DC power.

powers on the glass substrate. The transmittances of different samples in the wavelength range 200-800 nm. It was observed that by increasing the power value, the film transparency decreased. Most probably, the thicker film is denser and more defective, resulting in a decrease in film transparency. The films were 75 - 80% transmitting in the visible and ultraviolet range and had steep absorption edges at ≈ 250 nm. Hence the film deposited at 100 W is themost transparent in comparison to other films. The refractive index and thickness of the deposited films have been determined from their normal incidence transmission spectra by Swanepoel's method. [29]. Fig.7 shows both, the calculated and simulated refractive indices n for samples with different thickness. The experimental results are in good agreement with the results obtained using the Cauchy dispersion relation. The Cauchy dispersion relations for 100 W and 200 W are

$$n(100) = 1.56 + \frac{1.3 \times 10^4}{\lambda^2},$$
$$n(200) = 1.72 + \frac{1.6 \times 10^4}{\lambda^2}.$$
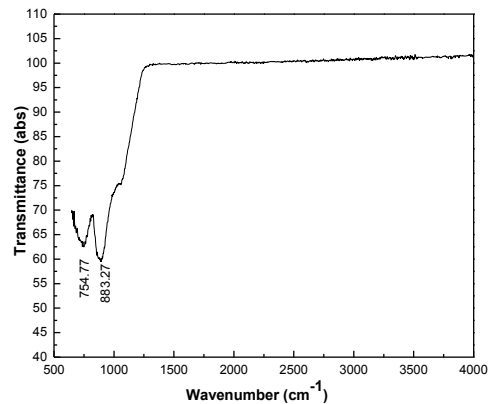

Figure 8. FTIR transmission spectra of AlN thin films deposited at 100 W.

Electrical resistivity (Ω-cm) and conductivity (Ω-cm^{-1}) measurement shown in Table 2 confirm that conductivity of 100W film is better than 400W films. It had been observed that conductivity of 300W and 400 W films are nearly in same range where as conductivity of 200W film is higher than these films. Electrical resistivity value of AlN varies in between 10^7 Ω cm to $10^{14}\Omega$ cm [39-41]. Thus the film prepared at 100W shows resistivity that falls in semiconductor range and films prepared at higher power shows properties like insulators.

Table 2: Electrical resistivity- conductivity of DC sputtered AlN films

DC Power (W)	Resistivity (Ω-cm)	Conductivity (Ω-cm^{-1})
100	8.1×10^4	1.2×10^{-5}
200	3.8×10^6	2.6×10^{-7}
300	2.3×10^8	1.9×10^{-9}
400	8.6×10^8	$\times 10^{-10}$

4. CONCLUSIONS

AlN thin films are grown on Si and glass substrates by DC magnetron sputtering in plasma containing a mixture of argon and nitrogen with different power. AFM results show that the grown films are smooth and dense. FTIR spectroscopy reveals that the formation of Al-N bond in the films and XRD patterns confirm that a preferred orientation of (100). The film optical properties have been investigated by Swanepoel's method.

The effect of DC power is investigated with respect to film thickness, surface roughness, and transmittance of AlN films. With increase in DC power, growth rate and the RMS surface roughness increases. AlN thin film deposited at 100 W have low surface roughness and high transparency in the visible spectra. The optical constants of the films, such as refractive index and extinction coefficient, are determined from optical transmittance by Swanepoel's method. The experimental values of refractive index are in good agreement with those obtained using the two- term Cauchy dispersion relation. Also, the optical results confirm the dependence of optical properties on the film thickness. A thicker film shows a higher refractive index. From the results, it is concluded that AlN thin films deposited at low DC power is a good candidate for optical device applications.

ACKNOWLEDGEMENTS

REFERENCES

[1] M Garcia Mendez, S Morales Rodriguez, R Machorro, W. De La Cruz, Mexicana De Fisica 54(4), (2008) 271.

[2] V.Dumitru, C.Morosanu, V.Sandu, A.Stoica, Thin Solid Films 359, (2000)17.

[3] R.Thapa, B. Saha, K.K.Chattopadhyay, Applied Surface Science 255, (2009) 4536.

[4] X.D.Wang, W.Jiang, M.G.Norton, K.W.Hipps, Thin Solid Films 251, (1994) 121.

[5] H.Morkoc, Springer, New York.17, (1999).

[6] I.Akasaki, H.Amano, Y.Koide, K. Hiramatsu, N.Suwaki, Journal of crystal growth 98, (1989) 209.

[7] K.Hiramatsu, S.Itoh, H.Amano, I.Akasaki, N.Kuwano, T.Shiraishi, K.oki J.Cryst. Growth 115, (1991) 628.

[8] L.F.Jiang, W Z Shen, H. Guo Qx, J. Appl Phys 94, (2003) 5704.

[9] Guo Qx, J Diang , T Tanaka, M Nishio, H.Ogawa, Appl.Phys. Lett. 86, (2005)111.

[10] Hsyi-En Cheng, Tien Chai Lin, Wen Chien-Chen, Thin Solid Films 425, (2003) 85.

[11] C. Caliendo, P. Imperaton, E. Cianci, Thin Solid Films 441, (2003) 32.

[12] J.P.Kar, G.Bose, S.Tuli Scripta Materials 54, (2006) 1755.

[13] Duy Thach Phan, Gwiy Sang Chung, Applied Surface Science 257, (2011) 8696.

[14] C.Mirpuri, S-Xu and J.D.Long, K.Ostrikov , J.Applied Physics 101, (2007) 024.

[15] Z R Song, Yuyh, Shen DS, Zousc, Zheng ZH, E Z Luo et.al Mater. Lett., 57, (2003) 4643.

[16] R.F. Davis, Proc of the IEEE,79, (1991) 702.

[17] J.E. Sungren, and H. Hentzel, J.Vac Sci Technol, A4, (1986) 2259.

[18] Y.Somno, M.Sasaki and T. llirai, Thin Solid Films 202, (1991) 333.

[19] W.M.Yim, E.J.Stofko, P.J.Zanzucchi, J.I.Pankove, M.Ettenberg and S.L.Gilbert. J.Appl.Phys 44, (1973) 292.

[20] M. Miyauchi, aay. Aishikawa, N.Shibata, Jpn J Appl.Phys. 31, (1992) L1714.

[21] E.Calleja, MASanchez Garcia, E Monroy, F J Sanchez E Munoz, A Sanz Hervas et.al., J. Appl. Phys. 82, (1997) 4681.

[22] C.Ristoscu, C.Ducu, G.Socol, F.Craciunoiu, I.N.Mihailescu, Applied Surface Sciences 248, (2005) 411.

[23] S.Six, J.W Gerlach, B.Rauschenbach, Thin Solid Films 370, (2000)1.

[24] R. D. Vispute, Wu H Narayan, Appl. Phys Lett. 67, (1995) 1549.

[25] M.Ishihara, H.Yumoto, T.Tsuchiya, K.Akashi, Thin Solid Films 281, (1996) 321.

[26] Xu Xiao-Hong, Wu Hai-Shun, Cong-Jie Zhang, Jin Zhi-Hao Thin Solid Films 388, (2001) 62.

[27] M. A. Auger, L.Vazguer, M. Jergel, O Sanchez, J.M Albella, Surface and Coating Technology. 180-181, (2004) 140.

[28] D.Poelman and P.F.Smet: J.Phys.D 36 (2003) 1850.

[29] R. Swanepoel, J.Phys. E 16, (1983) 1214.

[30] J.C.Manifacier, J.Gasiot, and J.P.Fillard: J.Phys. E 9, (1976) 1002.

[31] S.D.Ventura, E.G.Birgin, J.M.Martinez and I.Chambouleyron: J.Appy.Phys. 97, (2005) 043512.

[32] P.K. Barhai, Neelam Kumari, I. Banerjee, S.K. Pabi, S.K. Mahapatra, Vacuum 84, (2010) 896.

[33] F.A. Jenkins and H.E. White, Fundamentals of Optics (McGraw-Hill, New York, 1976) p. 479.

[34] J.C.Manifacier, J.Gasiot, and J.P.Fillard: J.Phys. E 10029 (1976).

[35] S. Z. Wu, Journal of Appl. Phy., 98, (2005) 083301.

[36] Y. Kajikawa , S Noda, H. Komiyama, J Vac. Sci Technol A 2003, (1943) 21.

[37] C Balasubramanian, S Bellucci, G Cinque, A Marcelli, M Cestelli Guidi, M Piccinini, A Popov, A Soldatov and P Onorato, J.Phys. Condens Matter. 18, (2006) S2095

[38] W Jonathan Vanbuskirk, T. Prokofyeva, M.Seon, A.S.Nikishin, H.Temkin, M.Holtz, S.Zollner, the Smithsonian/NASA Astrophysics Data system.

[39] X.Hou, K.Chou, X.Zhong and S.Seetharaman. Journal of Alloys and compounds. 465, (2008) 90.

[40] H.C.Barshilia, B.Deepthi and K.S.Rajam, Thin solid Films. (India). 516, (2008) 4168.

[41] J.Edwards, K.Kawabe, G.Stevens and R.H.Tredgold, Solid Communications 3, (1965) 99.